Variable linear polarization from an X-ray undulator

A. T. Young,[a]* E. Arenholz,[a] S. Marks,[a] R. Schlueter,[a] C. Steier,[a] H. A. Padmore,[a] A. P. Hitchcock[b] and D. G. Castner[c]

[a]Advanced Light Source Division, Lawrence Berkeley National Laboratory, Berkeley, CA 94720, USA, [b]Brockhouse Institute for Materials Research, McMaster University, Hamilton, ON, Canada L8S4M1, and [c]Department of Chemical Engineering, Box 351750, University of Washington, Seattle, WA 98195-1750, USA. E-mail: atyoung@lbl.gov

A new X-ray undulator has been designed and constructed which produces linearly polarized X-rays in which the plane of polarization can be oriented to a user selectable angle, from horizontal to vertical. Based on the Apple-II elliptically polarizing undulator (EPU), the undulator rotates the angle of the linear polarization by a simple longitudinal motion of the undulator magnets. Combined with the circular and elliptical polarization capabilities of the EPU operating in the standard mode, this new undulator produces soft X-ray radiation with versatile polarization control. This paper describes the magnetic structure of the device and presents an analysis of the magnetic field with varying undulator parameters. The variable linear polarization capability is then exhibited by measuring the X-ray absorption spectrum of an oriented polytetrafluoroethylene thin film. This experiment, which measures the linear dichroism of the sample at two peaks near the C 1*s* absorption edge, demonstrates the continuous polarization rotation capabilities of the undulator.

Keywords: undulators; variable linear polarization; linear dichroism; carbon NEXAFS.

1. Introduction

Synchrotron light sources have shown themselves to be invaluable research tools. One of the keys to their success as high-brightness sources of X-rays is the development of insertion devices. Using arrays of either electromagnets or permanent magnets, they create a periodic magnetic field, greatly increasing the flux and brightness of the X-rays produced (Kim, 1995; Schlueter, 1994; Elleaume, 1994). Most undulators to date have been planar types, either in a hybrid magnetic structure, combining permanent magnets with iron/steel pole tips, or in a pure permanent magnet structure. These devices produce horizontally linearly polarized light, with existing devices producing light from below 5 eV to beyond 60 keV over a range of storage ring energies.

In addition to these conventional undulators, a number of alternate designs have emerged. Most of these devices have special spectral or polarization properties. Among the most popular of these designs is the Apple-II or elliptically polarizing undulator (EPU) (Sasaki, 1994; Sasaki *et al.*, 1992; Carr & Lydia, 1993). These undulators, first developed by Sasaki, can produce light with a variety of polarizations, from linear horizontal to arbitrary elliptical/helical (both left and right) to linear vertical. Later, it was recognized (S. Sasaki, private communication) that linear polarization at angles other than horizontal and vertical could be generated, and an analysis of the operation to produce X-rays at 45°/135° has been published (Hwang & Yeh, 1999). The flexible polarization properties of this undulator design have led to their installation or planned inclusion at a number of synchrotrons around the world, including BESSY II (Senf *et al.*, 1998), the Swiss Light Source (Schmidt *et al.*, 2001), the Canadian Light Source (private communication), the Synchrotron Radiation Research Center (Chung *et al.*, 2001), the European Synchrotron Radiation Facility (Chavanne *et al.*, 2000) and the Pohang Light Source (Baek *et al.*, 2001).

At the Advanced Light Source, Lawrence Berkeley National Laboratory, we have designed and constructed a new undulator beamline, BL4.0.2, which is equipped with a 5 cm-period EPU and a high-spectral-resolution variable included-angle plane-grating monochromator. This beamline, with an energy range from 50 eV to 2000 eV, has been optimized for high-resolution spectroscopy on systems which exhibit polarization-dependent absorption in the soft X-ray energy range, including the *L*-edges of transition metals, *M*-edges of rare earths, and the carbon, nitrogen and oxygen *K*-edges. The initial performance of this beamline operating in the elliptical mode has been described elsewhere (Young *et al.*, 2001). We have now also developed a new operating mode of the EPU in which linearly polarized light is generated, but with the plane of polarization rotated from horizontal. Rotation angles can be varied continuously, from 0° to 90°, *i.e.* rotation from horizontal to vertical, and are obtained under full user control.

This paper describes the magnetic design of the EPU, showing how the varying magnetic fields are generated. We then describe experiments to demonstrate the polarization rotation using an oriented polytetrafluoroethylene (PTFE) film as the sample. The linear dichroism of this sample is measured using both sample rotation and polarization rotation, showing that continuously tunable variable linear polarization in generated.

2. Magnetic structure of the EPU

The magnetic design of the EPU has been described previously (Marks *et al.*, 1998) and is shown schematically in Fig. 1. A pure permanent magnet device, it has an upper and lower jaw. As in conventional undulators, the strength of the on-axis magnetic field, and therefore the photon energy, is controlled by changing the vertical gap between the jaws. Unlike conventional undulators though, each jaw is split in half lengthwise, creating a magnetic structure with four quadrants. For each quadrant, each period of the device is made up of four blocks of magnetic material with the magnetization directions oriented differently, as shown in Fig. 1. Moving the quadrants longitudinally changes the on-axis magnetic field of the device, which changes both the energy and the polarization state of the X-rays.

The standard method of operation for these Apple-II-type EPUs is to move a diagonal pair (*e.g.* quadrants 2 and 4) of the magnet rows longitudinally (along the z axis) in the same direction. This 'parallel' mode of operation generates a magnetic field in which the x and y components (where y is vertical and x is transverse to the undulator axis) of the magnetic field (B_x and B_y) are 90° out of phase, creating an elliptical/helical magnetic field. Passage of the stored electron beam through this field produces elliptically or circularly polarized X-rays. The magnitudes of B_x and B_y are determined by both the gap and the z shift, or phase, of the magnet rows, so that control of the energy and polarization requires both gap and phase control of the undulator. When the shift of the quadrants is zero, the field has only a B_y component and the radiation is linearly polarized horizontally. If the shift is $\lambda/2$, where λ is the period length of the undulator, the field has only a B_x component and the radiation is linearly polarized vertically.

The new mode of operation requires that the members of the diagonal pair move in opposite directions, *e.g.* quadrant 2 moves a distance $+\Delta z$, while quadrant 4 moves $-\Delta z$. We term this new scheme of operation the antiparallel mode. In this mode, B_x and B_y remain in phase, and linear polarization is generated. B_x and B_y are still dependent upon the gap and the phase, so the angle of the polarization can be controlled by varying these two parameters. This can be seen in the following analysis.

Consider the magnetic field generated by a single quadrant. The variation of this field as measured on the axis of the undulator is

$$B_{qx}(z) = -b_{qx_o}\cos(kz) \qquad \text{quadrants 1 and 3}, \tag{1a}$$

$$B_{qx}(z) = b_{qx_o}\cos(kz) \qquad \text{quadrants 2 and 4}, \tag{1b}$$

$$B_{qy}(z) = b_{qy_o}\cos(kz), \tag{2}$$

where b_{qx_o} and b_{qy_o} are the amplitudes of the x and y components of the on-axis field generated by a single quadrant, λ is the period of the undulator, z is along the axis of the undulator and $k = 2\pi/\lambda$.

If we translate a quadrant by a distance Δz and define the row phase change $\varphi = 2\pi\Delta z/\lambda$ we obtain

$$B_{qx}(z) = -b_{qx_o}\cos(kz-\varphi) \qquad \text{quadrants 1 and 3}, \tag{3a}$$

$$B_{qx}(z) = b_{qx_o}\cos(kz-\varphi) \qquad \text{quadrants 2 and 4}, \tag{3b}$$

$$B_{qy}(z) = b_{qy_o}\cos(kz-\varphi). \tag{4}$$

For the ALS EPU, quadrants 1 and 3 are stationary while 2 and 4 translate. The net field from all four quadrants is then

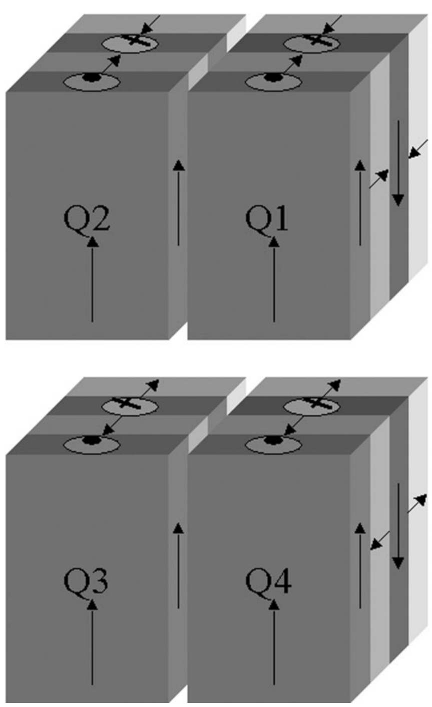

Figure 1
Schematic magnetic design of the EPU. Quadrants 2 and 4 move longitudinally, in and out of the plane of the figure. Moving the quadrants in the same direction (parallel mode) yields elliptically polarized light, while moving them in the opposite direction (antiparallel mode) produces linearly polarized light at varying angles.

$$B_x(z) = b_{qx_o}\left[-2\cos(kz) + \cos(kz-\varphi_2) + \cos(kz-\varphi_4)\right], \tag{5}$$

$$B_y(z) = b_{qy_o}\left[2\cos(kz) + \cos(kz-\varphi_2) + \cos(kz-\varphi_4)\right], \tag{6}$$

where φ_2 and φ_4 are the row phase changes for quadrants 2 and 4.

If $\varphi_2 = -\varphi_4 \cong \varphi$, that is, we move the quadrants in the antiparallel mode, we obtain

$$B_x(z) = 2b_{qx_o}[\cos(\varphi) - 1]\cos(kz) = B_{x_o}\cos(kz), \tag{7}$$

$$B_y(z) = 2b_{qy_o}[\cos(\varphi) + 1]\cos(kz) = B_{y_o}\cos(kz). \tag{8}$$

Therefore, B_x and B_y are in phase and the radiation will be linearly polarized at an angle θ,

$$\theta = \tan^{-1}\left[\frac{-b_{qx_o}}{b_{qy_o}}\frac{\cos(\varphi)-1}{\cos(\varphi)+1}\right]. \tag{9}$$

The photon energy is determined from

$$\varepsilon\ (\text{eV}) = 950\,E^2/\left\{\left[1 + \left(K^2/2\right)\right]\lambda\right\}, \tag{10}$$

where E is the electron beam energy in GeV, λ is the undulator period in cm, and K is given by

$$K = 0.934\lambda\left(B_{x_o}^2 + B_{y_o}^2\right)^{1/2}, \tag{11}$$

where the magnetic field is given in Teslas.

Note that b_{qx_o} and b_{qy_o} are gap-dependent. This means that the polarization rotation angle θ depends on both the row phase change φ and the vertical undulator gap. Experiments with constant photon energy and a varying polarization angle therefore need to have both the row phase and vertical gap varying and synchronized. Similarly, as the photon energy ε is a function of B_{x_o} and B_{y_o}, it also depends on both the gap and the row phase. Therefore, experiments at a constant polarization angle and a varying photon energy also need to have the row phase and vertical gap synchronized.

Fig. 2 illustrates the behavior of the polarization rotation angle with row phase change at two different gaps. Parameters for the calculations are those of the ALS EPU at beamline 4.0.2, *e.g.* a beam energy of 1.9 GeV and a period of 5 cm. The different rotation angles

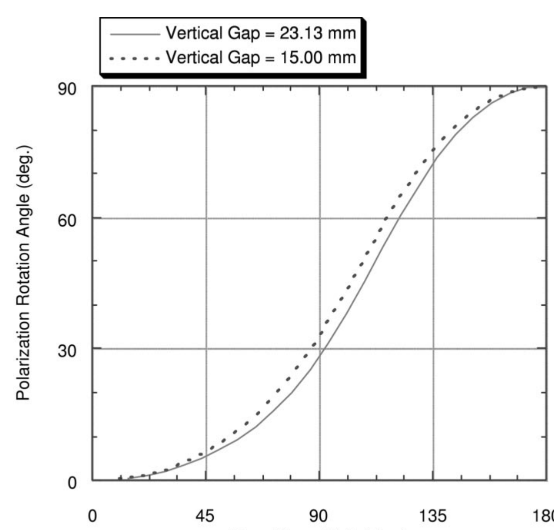

Figure 2
The linear polarization angle as a function of the magnet row phase for two different vertical gaps. The polarization angle is dependent upon both the row phase and the gap.

for the same row phase shift reflects the fact that the ratio b_{qx_o}/b_{qy_o} is not constant with gap. Fig. 3 shows the behavior of the photon energy under the same conditions. Note that for fixed gap the photon energy does not change monotonically with row phase. Also, by looking at the calculation for the smallest vertical gap, 14.9 mm, we see that the minimum energy for which all polarization angles can be generated is 215 eV, compared with 83.3 eV and 168 eV, the minimum energies for horizontal and vertical polarizations, respectively.

3. Experimental

To confirm the rotation of the polarization angle with row phase, the near-edge absorption spectrum of an oriented polymer was studied. The experiments were performed at BL4.0.2 at the ALS. Measurements of the photon energy as a function of vertical gap for linear horizontal and linear vertical polarization yielded the values for b_{qy_o} and b_{qx_o}, from which tables of undulator gap and phase for arbitrary polarization angle and energy were generated. The ALS control system includes both fast (200 Hz) orbit feedforward and slow (1 Hz) orbit feedback to keep the orbit stable under all configurations of the undulator. This allows for user control of both the gap and the phase under normal operating conditions, providing experimenters with total control of the photon energy and polarization (Steier *et al.*, 2000). Scans with varying energy at fixed polarization or with varying polarization angle at fixed energy can be obtained using the beamline control system, which synchronizes the undulator configuration with the monochromator settings. All measurements described were made using the fundamental output of the undulator. Higher energies can be obtained by using the third- or fifth-harmonic output.

An oriented polymer film was produced by rubbing PTFE on a hot substrate, in our case a silicon wafer. The CF_2 polymer chains align along the direction of the rubbing and the substrate is then cooled to room temperature. The sample was mounted on a rotary feedthrough whose axis is coincident with the photon beam. With the sample mounted perpendicular to the axis, rotation of the feedthrough (*i.e.* variation of the azimuthal angle of the sample) rotates the direction of the polymer chains with respect to the plane of the polarization. Absorption spectra near the carbon *K*-edge were obtained by measuring the sample current from the film as a function of photon energy at fixed polarization and sample orientation angles. Sample current measurements were also taken at fixed photon energies while varying either the polarization angle or the sample orientation angle.

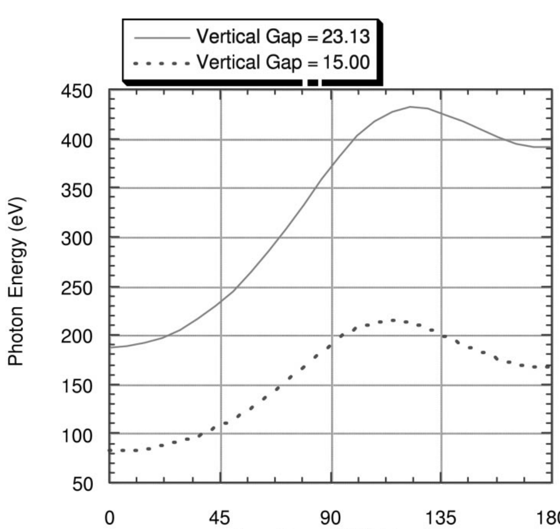

Figure 3
Photon energy as a function of the magnet row phase for two different gaps.

4. Results and discussion

Previous work (Castner *et al.*, 1993; Ishii *et al.*, 1988) has shown that the carbon *K*-edge absorption spectrum consists of two major components: a lower-energy peak at 292.2 eV of $\sigma^*_{\rm C-F}$ character, which arises from C 1*s* excitations to sp^3 orbitals oriented mostly perpendicular to the polymer backbone; and a higher-energy peak at 295.6 eV, which originates from C 1*s* excitations to $\sigma^*_{\rm C-C}$ orbitals aligned mostly along the backbone. These two peaks exhibit linear dichroism, that is, the absorption signal is dependent on the polarization orientation of the incident X-rays. The peak at 292.2 eV is a maximum when the polarization is perpendicular to the polymer backbone, while the peak at 295.6 eV is a maximum when the polarization is parallel to the polymer backbone. Fig. 4 shows measured near-edge X-ray absorption fine-structure (NEXAFS) spectra of the polymer sample obtained with the undulator set to produce linear polarization at three different angles, 0° (horizontal), 45° and 90° (vertical). For these measurements, the orientation of the rubbing direction of the polymer (along which the chains are aligned) was horizontal, *i.e.* at 0°. As can be seen, when the polarization angle is 0°, the 292.2 eV peak is small and the 295.6 eV peak is large, whereas when the polarization angle is 90°, the 292.2 eV peak is large and the 295.6 eV peak is small. When the polarization angle is 45°, the peaks have amplitudes that are between the extremes. Fig. 4(*d*) was recorded with the polarization angle at 45°, but with the sample rotated by −45°, producing a net angle between the polarization and the polymer orientation of 90°. This spectrum is almost identical to the 90° polarization/0° sample position spectrum, as expected.

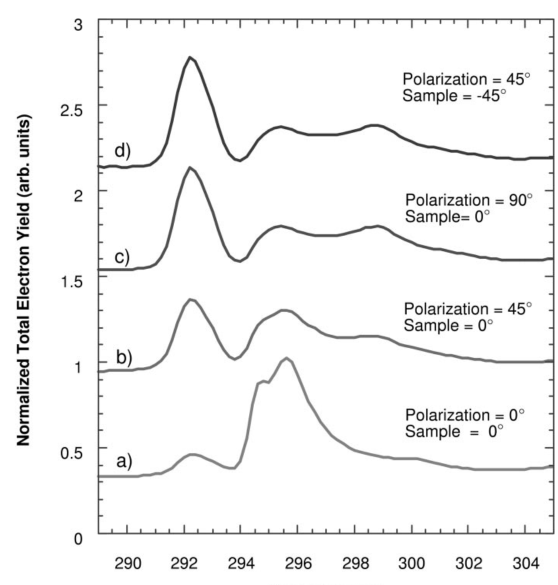

Figure 4
Absorption spectra of an oriented PTFE film near the carbon *K*-edge at different polarization and sample angles. [A polarization angle of 0° corresponds to the *E* vector in the plane of the storage ring; a sample angle of 0° corresponds to the PTFE chains (rubbing direction) being aligned with the plane of the storage ring.] The spectra have been normalized to the same C 1*s* intensity at 304 eV. Offsets of (*b*) 0.5, (*c*) 1.0 and (*d*) 1.5 have been used for clarity.

Fig. 5 further demonstrates the polarization rotation capabilities of the ALS EPU. Each curve is a measurement of the sample current as a function of the azimuthal angle of the sample. The curves are measurements taken with different polarization angles. The photon energy is 292.2 eV, the energy of the $\sigma^*_{\rm C-F}$ peak. The solid line in Fig. 5 shows the signal with a polarization angle of 0°, *i.e.* linear horizontal. The intensity is cyclic with a period of 180°, as expected since the absorption intensity should be proportional to $\sin^2\alpha$, where α is the angle between the plane of polarization and the oriented polymer chains. The dotted line is a similar sample rotation measurement, but in this case the row phase of the EPU has been set (Δz = 15 mm) to rotate the angle of the linear polarization by about 45°. Note that the sample signal still oscillates with the 180° period, but the maximum is shifted by 45°. Finally, with Δz = 25 mm, the polarization is rotated by another 45°, giving vertically linearly polarized X-rays. The sample signal again shows the same cyclic variation with rotation but is shifted by 90° from the Δz = 0 data, as expected.

Finally, Fig. 6 shows the results of scanning the polarization angle from 0° to 90°, for several sample orientation angles and at fixed photon energy. For each orientation of the sample, the polarization angle scans show a maximum. The position of the maximum moves in angle along with the sample orientation angle. The first five curves were obtained at 292.2 eV at sample angles of 0°, 15°, 35°, 45° and 60°, while the last curve was obtained at 295.6 eV at a sample angle of 35°. As expected, it shows the opposite behavior from the 292.2 eV/35° orientation spectrum, as the $\sigma^*_{\rm C-C}$ transition exhibits the opposite linear dichroism of the $\sigma^*_{\rm C-F}$ transition.

The ability to rotate the linear polarization to an arbitrary angle provides an additional degree of freedom to experimental design. Although variation of the angle between the sample orientation and the polarization vector can be accomplished by a simple rotation of the sample, there are situations in which it is difficult or impossible to achieve the desired polarization–sample–detector geometries. Examples include some angle-resolved photoemission experiments, full-field photoemission electron microscopy, and scanning transmission X-ray microscope systems. In the case of X-ray microscopies, the stability requirements are very stringent so it is difficult or impossible to carry out azimuthal sample rotations while leaving the same point on the sample under the incident photon beam. Also, rotating the sample can change the aspect ratio of the illuminated spot on the sample, creating a possible source of error. Thus, the ability to rotate the polarization vector greatly simplifies experiments that heretofore have been either impossible or very difficult to perform.

A practical consideration is whether or not the variable linear polarization mode adversely affects the stored electron beam. When operated in this mode, the undulator influences the beam in several different ways. The largest effects are closed-orbit distortions. The fast (200 Hz) orbit feedforward and slow (1 Hz) orbit feedback keep the orbit stable under all configurations of the undulator, including the variable linear polarization mode. Other sizeable effects include changes in the linear betatron tunes, the linear chromaticites and linear coupling, while effects due to higher multipole components are negligible. These can all influence the vertical beam size but, in our case, are small enough that they do not additionally affect the nonlinear dynamics in any significant way (*e.g.* lifetime, injection efficiency). Correction schemes to minimize the effects on the vertical beam size are planned. The magnitudes of all these effects in the new mode are about the same as in the parallel mode.

This new operating mode of the Apple-II EPUs boosts the versatility of the design. Such a device has full polarization control, with the ability to generate both left- and right-circularly polarized radiation and linear polarization at arbitrary angles. However, it does require that the mechanical design of the device be such that the moving quadrants can be moved in opposite (antiparallel) directions as well as in the same (parallel) direction, which is the mode used to generate elliptically polarized light.

The mechanical design also needs to accommodate the additional forces placed on the support structure that are not present when the rows are moved in the same direction. The major difference in the forces between the two operating modes is that the variable linear

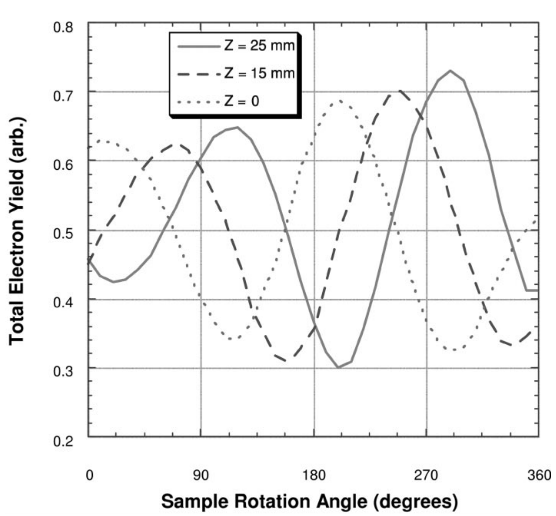

Figure 5
Rotation of the PTFE sample angle at fixed polarization angles. The photon energy is 292.2 eV, the $\sigma^*_{\rm C-F}$ transition. The three measurements correspond to the polarization angles of 0° (z = 0 mm), 45° (z = 15 mm) and 90° (z = 25 mm). As the polarization angle is changed, the sample angle positions of maximum signal change by the same amount.

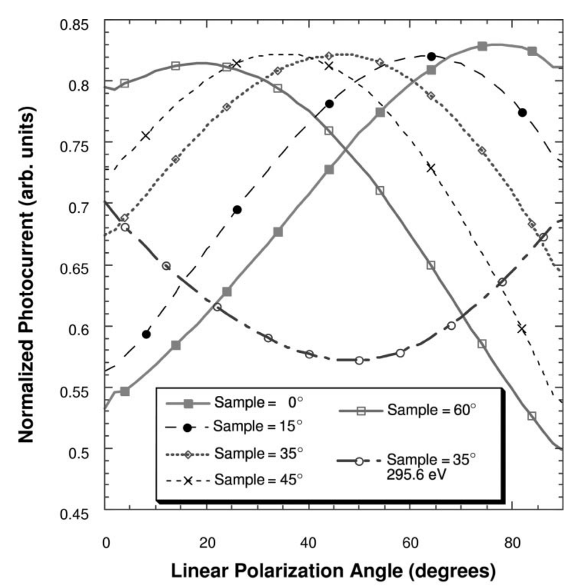

Figure 6
Variation of the polarization angle at fixed PTFE sample orientation angles. The first five measurements were taken at a photon energy of 292.2 eV, the $\sigma^*_{\rm C-F}$ transition. As the polarization angle is changed, the signal goes through a maximum when the electric field vector is aligned with the transition dipole. As the sample orientation is changed, the polarization angle for maximum signal changes by the same amount. The measurement at 295.6 eV, the $\sigma^*_{\rm C-C}$ transition, shows the opposite linear dichroism.

mode produces torques in both the xz plane [quadrants 2 and 3 have a force driving them forward ($+z$) while quadrants 1 and 4 are forced backward ($-z$)] and in the yz plane [quadrants 2 and 3 have an upward ($+y$) force and quadrants 1 and 4 have a downward ($-y$) force]. The magnitudes of these forces, as well as the F_x and F_z forces in the elliptical mode, are sensitive to the spacing between the quadrants on each jaw (*i.e.* the small clearances between quadrants 1 and 2 on the upper jaw and between quadrants 3 and 4 on the lower jaw). For the ALS EPU, the spacing is nominally 1.0 mm, with a minimum spacing of 0.5 mm. This gives rise to forces which, under all operating conditions, are <10000 lbs.

5. Summary

The generation of linearly polarized X-rays with an adjustable angle of polarization has been demonstrated for the first time in an APPLE-II-type undulator. By operating the undulator quadrants in an antiparallel mode, rotation of the plane of polarization between horizontal and vertical is easily accomplished. This new operating mode of the EPU will make many linear-polarization-sensitive experiments much easier to perform, including angle-resolved photoemission and fluorescence experiments, studies of magnetic linear dichroism, and photoemission and scanning transmission X-ray microscopy.

This work was supported by the Director, Office of Energy Research, Office of Basic Energy Sciences, Materials Science Division, of the US Department of Energy under Contract No. DE-AC03-76SF00098. DGC acknowledges support from NIH grant RR-01296.

References

Baek, I.-G., Kim, J.-Y. & Oh, S.-J. (2001). *Nucl. Instrum. Methods*, A**467**/**468**, 545–548.

Carr, R. & Lydia, S. (1993). *Proc. SPIE*, **2013**, 56.

Castner, D. G., Lewis, K. B., Fischer, D. A., Ratner, B. D. & Gland, J. L. (1993). *Langmuir*, **9**, 537–542.

Chavanne, J., Van Vaerenbergh, P., Elleaume, P. & Gunzel, T. (2000). *Proceedings of the 7th European Particle Accelerator Conference (EPAC 2000)*, p. 2346. Vienna: Austrian Academy of Sciences.

Chung, S.-C., Huang, L-R., Chen, C.-C., Cheng, N.-F., Chuang, J. M., Tseng, P.-C., Huang, D. J., Lin, H. J., Chen, J., Perng, S.-Y., Chen, C. T. & Tsang, K.-L. (2001). *Nucl. Instrum. Methods*, A**467**/**468**, 445–448.

Elleaume, P. (1994). *J. Synchrotron Rad.* **1**, 19–26.

Hwang, C. S. & Yeh, S. (1999). *Nucl. Instrum. Methods*, A**420**, 29.

Ishii, I., McLaren, R., Hitchcock, A. P., Jordan, K. D., Choi, H. & Robin, M. B. (1988). *Can. J. Chem.* **66**, 2104–2121.

Kim, K.-J. (1995). *Opt. Eng.* **34**, 342.

Marks, S., Cortopassi, C., DeVries, J., Hoyer, E., Leinbach, R, Minamihara, Y., Padmore, H., Pipersky, P., Plate, D., Schlueter, R. & Young, A. (1998). *Proceedings of the 1997 Particle Accelerator Conference*, edited by M. Comyn, M. K. Craddock, M. Reiser & J. Thomson, pp. 3221–3223. Piscataway, NJ: IEEE.

Sasaki, S. (1994). *Nucl. Instrum. Methods*, A**347**, 83.

Sasaki, S., Miyata, K. & Takada, T. (1992). *Jpn. J. Appl. Phys.* **31**, L1794.

Schlueter, R. D. (1994). *Wiggler and Undulator Insertion Devices* in *Synchrotron Radiation Sources – A Primer*, edited by H. Winick. River Edge, NJ: World Scientific.

Schmidt, T., Ingold, G., Imhof A., Patterson, B. D., Patthey, L., Quitmann, C., Schulze-Briese, C. & Abela, R. (2001). *Nucl. Instrum. Methods*, A**467**/**468**, 126–129.

Senf, F., Sawhney, K. J. S., Follath, R., Scheer, M., Schafers, F., Bahrdt, J., Gaupp, A. & Gudat, W. (1998). *J. Synchrotron Rad.* **5**, 747–749.

Steier, C., Portmann, G. & Young, A. T. (2000). *Proceedings of the 7th European Particle Accelerator Conference*, edited by J.-L. Laclare, W. Mitaroff, Ch. Petit-Jean-Genaz, J. Poole & M. Regler, p. 2343. Vienna: Austrian Academy of Sciences.

Young, A. T., Arenholz, E., Feng, J., Padmore, H. A., Henderson, T., Marks, S., Hoyer, E., Schlueter, R., Kortright, J. B., Martynov, V., Steier, C. & Portmann, G. (2001). *Nucl. Instrum. Methods*, A**467**/**468**, 549–552.

 Received 12 December 2001 • Accepted 18 April 2002